

# Applications of TG-FTIR: From Polymers to Pharmaceuticals, Foods, and Inorganic Materials

Yoshinobu Hosoi\*

## Abstract

TG-FTIR, which combines Simultaneous Thermal Analysis (STA) consisting of Thermogravimetry (TG) and Differential Thermal Analysis (DTA) with Fourier Transform Infrared Spectroscopy (FTIR), is an effective method for simultaneously obtaining information about the reactions occurring in a sample upon heating and the resulting reaction products. This paper presents several applications of TG-FTIR in the analysis of polymers, pharmaceuticals, foods, and inorganic materials. In fiber-reinforced plastics (FRPs), bisphenol A is evolved under thermal decomposition, while CO<sub>2</sub> is released during combustion. For other polymers, H<sub>2</sub>O and CO<sub>2</sub> were quantified during combustion. TG-FTIR was also applied to simulate the ceramic debinding process and identify polymer plasticizers. Additionally, TG-FTIR proved effective in analyzing dehydration in pharmaceuticals, thermal oxidation of edible oils, and reactions in inorganic materials such as gypsum dihydrate.

## 1. Introduction

STA is an essential tool for reaction analysis, as it allows us to characterize reactions during heating or cooling by analyzing TG and DTA curves. However, it does not provide information about the substances yielded by these reactions. Combining STA with FTIR, known as TG-FTIR, effectively addresses this issue by enabling evolved gas analysis during mass losses upon heating samples<sup>(1),(2)</sup>. The TG-FTIR instrument shown in Fig. 1 consists of an STA furnace, a transfer line, and an FTIR gas cell. Reaction products evolved from the sample upon heating in the furnace are transported to the FTIR gas cell through the transfer line, which is heated to prevent condensation. This setup allows for real-time analysis of reaction products. The details of the instrument have been described in previous reports<sup>(2)</sup>. This paper introduces several applications of TG-FTIR, from polymers, pharmaceuticals, and foods to inorganic materials.



Fig. 1. Appearance of TG-FTIR.

\* Application Laboratories, Product Division, Rigaku Corporation.

## 2. Polymers

### 2.1. Decomposition and Combustion of FRPs

FRPs are composite materials consisting of a polymer matrix with reinforcing fibers. These fibers, which can be made of glass, carbon, aramid, or other materials, provide strength and stiffness to the composite. The polymer matrix is usually a thermosetting resin like epoxy, polyester, or vinyl ester. Advantages of FRP, including their light weight, high strength, and corrosion resistance, make them useful in various fields such as marine, aerospace, and automotive. As with all polymer products, the environmental impact of FRP production and disposal is a concern, driving the need for sustainable practices. Several studies have discussed the decomposition and combustion mechanisms of FRPs to improve the recyclability these materials<sup>(3)-(7)</sup>. TG-FTIR can evaluate the thermal decomposition and combustion processes of glass fiber-reinforced plastic (GFRP).

Figure 2 shows the TG-FTIR results with sample observation. When the black GFRP was heated in N<sub>2</sub> atmosphere, a 28% mass loss was initiated at around 400°C due to thermal decomposition of the polymer matrix. Carbonization also progressed concurrently with the thermal decomposition, although significant changes in the optical image were not observed due to the black color of the sample. As shown in Fig. 2(b), bisphenol A was detected by FTIR, indicating that epoxy resin was used for the polymer matrix.

Subsequently, the programmed temperature was held at 700°C, and the atmosphere was switched from N<sub>2</sub> to dry air. A sharp exothermic peak was observed along with a 3% mass loss. As shown in Fig. 2(c), the carbonized residue combusted, leaving behind only the glass fibers. CO<sub>2</sub> was detected in the IR spectrum, which also serves as evidence of combustion.

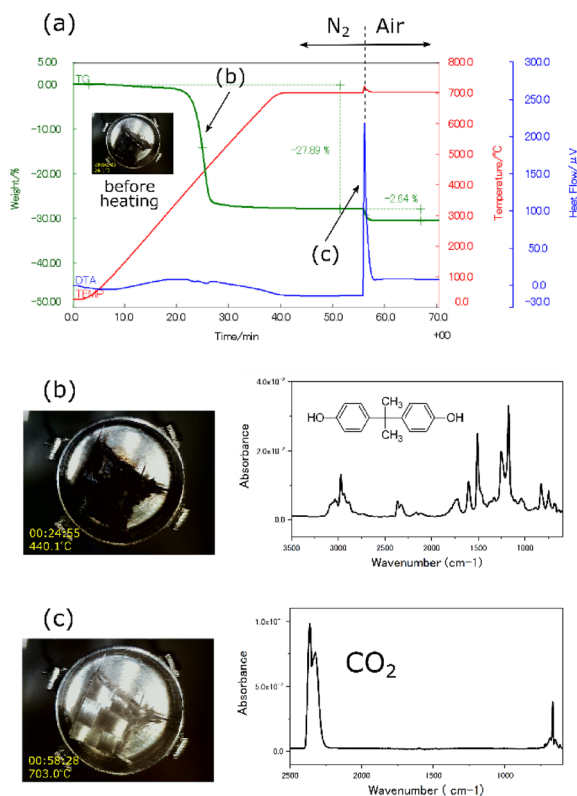


**Fig. 2.** TG-FTIR results of GPRP with sample observation: (a) TG-DTA, (b) sample observation image and IR spectrum at 440°C, (c) sample observation image and IR spectrum when switching atmosphere from N<sub>2</sub> to dry air.

### 2.2. Quantification of H<sub>2</sub>O and CO<sub>2</sub> Evolved During Polymer Combustion

There are two advantages to utilizing TG-FTIR for the quantification of evolved gases. Firstly, the signal intensity remains unaffected by changes in the atmosphere. In contrast, TG-MS, which is frequently compared to TG-FTIR, exhibits fluctuations in signal intensity of evolved gases depending on the atmospheric conditions. The TG-FTIR measurement can continue even if the atmosphere is changed during the measurement, as shown in section 2.1.

The other advantage is the stability of the signal intensity. In TG-FTIR, all evolved gases are introduced into the gas cell, and the optical path length of the gas cell is fixed. Consequently, the IR spectral intensity of the evolved gases remains constant relative to their quantity. In this study, H<sub>2</sub>O and CO<sub>2</sub> evolved during polymer combustion were quantified using calcium oxalate monohydrate as a calibration standard, which demonstrates stoichiometric evolution through dehydration and decarboxylation.

Figure 3 shows the results of TG-FTIR measurements when high-density polyethylene (HDPE) was heated in an air atmosphere. A mass loss and an exothermic peak were observed in the TG and DTA curves starting at 350°C. During this mass loss, the IR spectrum revealed peaks for H<sub>2</sub>O and CO<sub>2</sub>, confirming that the thermal decomposition gases of HDPE were converted to H<sub>2</sub>O

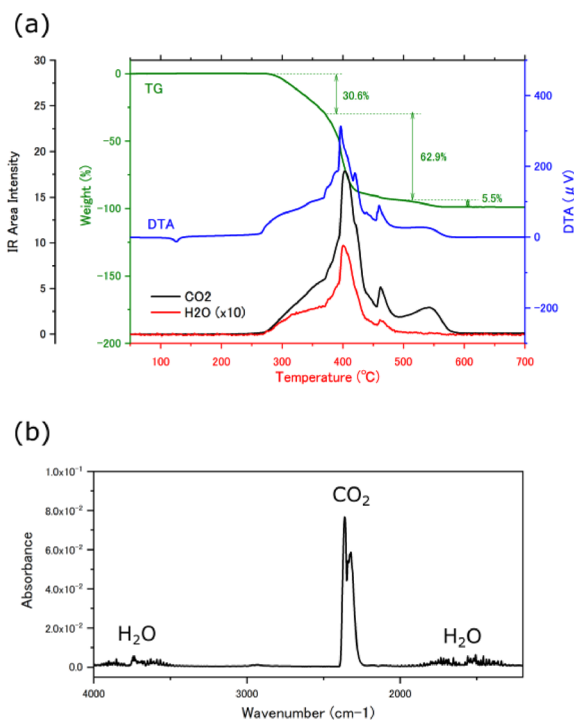


**Fig. 3.** (a) TG-DTA and temperature profiles of the area intensity of IR absorption bands of H<sub>2</sub>O and CO<sub>2</sub> of HDPE, (b) IR spectrum around 400°C.

**Table 1.** Evolution of H<sub>2</sub>O and CO<sub>2</sub> during combustion of each polymer.

Samples	H <sub>2</sub> O evolution / %	CO <sub>2</sub> evolution / %
<b>HDPE</b>	78	138
<b>PVC</b>	26	102
<b>Nylon 6</b>	63	136
<b>PS</b>	8	34
<b>PMMA</b>	15	38
<b>PET</b>	20	104
<b>PPS</b>	32	160
<b>Cellulose</b>	32	70
<b>Carbon Black</b>	N.D.	242

and CO<sub>2</sub> through combustion. The temperature profiles in the area intensity of the IR absorption bands of H<sub>2</sub>O and CO<sub>2</sub> corresponded with the mass loss in TG and the exothermic peaks in DTA. Quantification of the peak areas of the temperature profiles of H<sub>2</sub>O and CO<sub>2</sub>, using a calibration curve created with calcium oxalate monohydrate, revealed that 78% of H<sub>2</sub>O and 138% of CO<sub>2</sub> were evolved relative to the initial mass of HDPE.

Table 1 summarizes the quantitative results of H<sub>2</sub>O and CO<sub>2</sub> evolution during combustion of various polymers. These data can be effectively utilized to estimate the amount of CO<sub>2</sub> emissions during the incineration of plastic waste<sup>(8)</sup>.

### 2.3. Simulation of Debinding

Polyvinyl butyral (PVB) exhibits excellent dispersibility

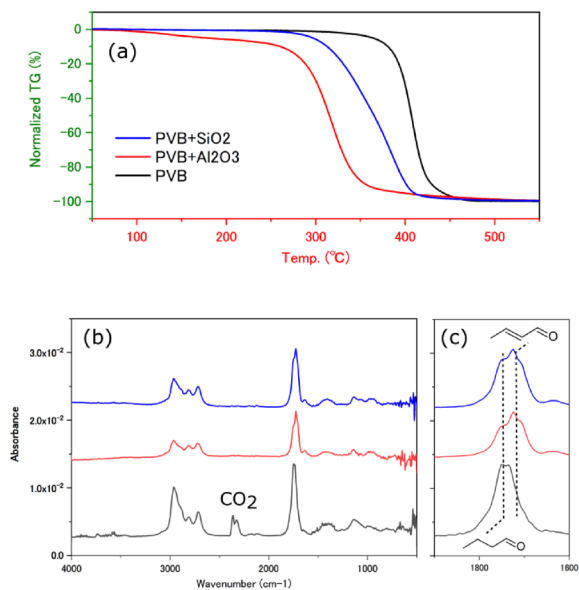


**Fig. 4.** TG-FTIR measurement of pristine PVB and its mixtures with SiO<sub>2</sub> and Al<sub>2</sub>O<sub>3</sub>. (a) TG, (b) IR spectra, (c) IR spectra magnified in the wavenumber region around 1700 cm<sup>-1</sup>.

of inorganic materials and is widely utilized as a ceramic binder. Consequently, numerous studies have employed TG-FTIR to investigate the thermal decomposition of PVB binders<sup>(9),(10)</sup>. In this study, we simulated the debinding process by heating samples of PVB alone and PVB with dispersed alumina and silica. Figure 4(a) shows the TG curves of each sample heated under N<sub>2</sub> atmosphere. Compared to PVB alone, the mixtures began to lose mass at a lower temperature. Figure 4(b) shows the IR spectra of the evolved gases during the mass loss. A CO<sub>2</sub> band was observed in the thermal decomposition of PVB alone, while it was absent in the mixtures. A minute difference was observed in the region around 1700 cm<sup>-1</sup> due to the carbonyl group, magnified in Fig. 4(c). The carbonyl group absorption band observed in PVB alone is assigned to butyraldehyde. A shoulder band on the low wavenumber side was observed in the mixtures, potentially contributing to 2-butenal. We concluded that the incorporation of inorganic substances into PVB results in the lower decomposition temperature and the alteration of the decomposition products.

## 2.4. Detection of Additives

TG-FTIR can be utilized to analyze not only polymers but also additives<sup>(11),(12)</sup>. Figure 5 presents the TG-FTIR measurements when a sample of polyvinyl chloride (PVC) with the plasticizer Di(2-ethylhexyl) phthalate (DEHP) was heated in N<sub>2</sub> atmosphere. A mass loss was observed between 200 and 350°C in the TG curve, as shown in Fig. 5(a). The Gram-Schmidt (GS) curve, which profiles the thermal behavior of the total evolved gases, exhibited two peaks at 280°C and 300°C. The IR spectra at these peak temperatures are shown in Fig. 5(b). The spectrum at 280°C is attributed to DEHP and CO<sub>2</sub>. In addition to these gases, HCl, which is a

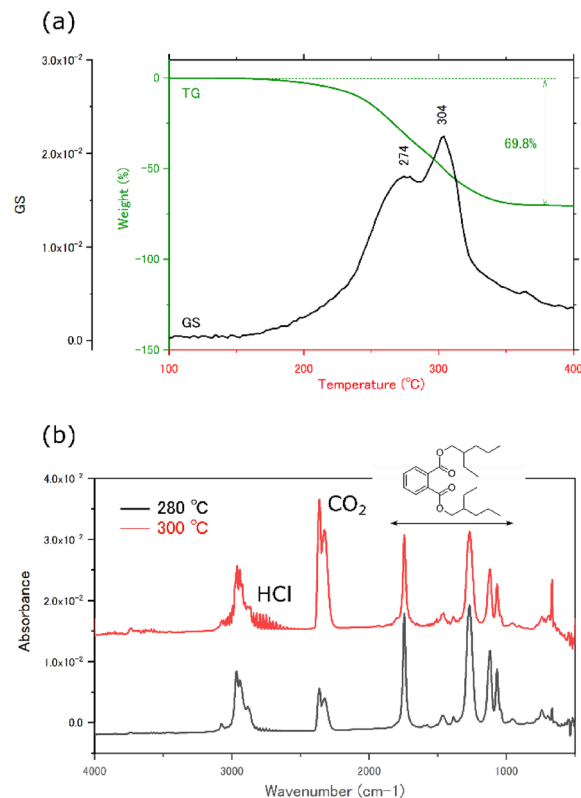


**Fig. 5.** TG-FTIR measurement of DEHP in PVC. (a) TG and GS curves, (b) IR spectra at 280 and 300°C.

decomposition product of PVC, was detected at 300°C. Upon heating this sample, the plasticizer DEHP desorbs first, followed by the thermal decomposition of PVC.

## 3. Pharmaceuticals and Foods

### 3.1. Desolvation of Pharmaceuticals

The desolvation of pharmaceuticals is a typical application of TG-FTIR. As stipulated in the Japanese Pharmacopoeia, TG is used as a method for testing loss on drying (LOD), providing information on mass losses at specific temperatures. However, TG cannot identify the substances evolved during the mass loss. Hyphenated FTIR can characterize the evolved gases<sup>(13)</sup>. Figure 6 shows the TG-DTA measurement when trehalose dihydrate is heated under N<sub>2</sub> atmosphere. A 9.3% mass loss and two endothermic peaks were observed below 200°C. The FTIR analysis of the evolved gases during the mass loss identified it as H<sub>2</sub>O (not shown in Fig. 6). A profile of H<sub>2</sub>O evolution behavior was obtained by plotting the temperature change in the area intensity of the IR absorption bands for H<sub>2</sub>O, corresponding to the mass loss. This indicates the dehydration of trehalose dihydrate, which is stoichiometrically consistent with the mass loss.

### 3.2. Thermal Oxidation of Edible Oils

Edible oils undergo oxidation by atmospheric oxygen, a process that is significantly accelerated at high temperatures. This deterioration, known as thermal oxidation, results in a loss of flavor and

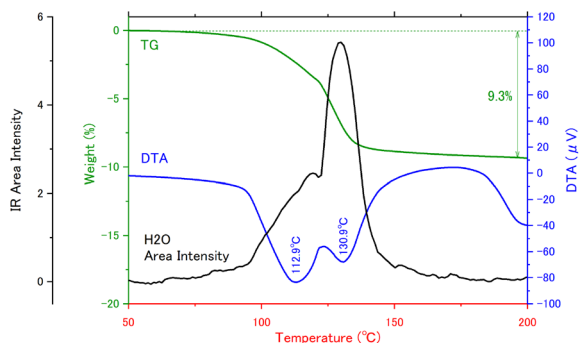


**Fig. 6.** TG-DTA of trehalose dihydrate and thermal profile of area intensity for the IR band assigned to H<sub>2</sub>O.

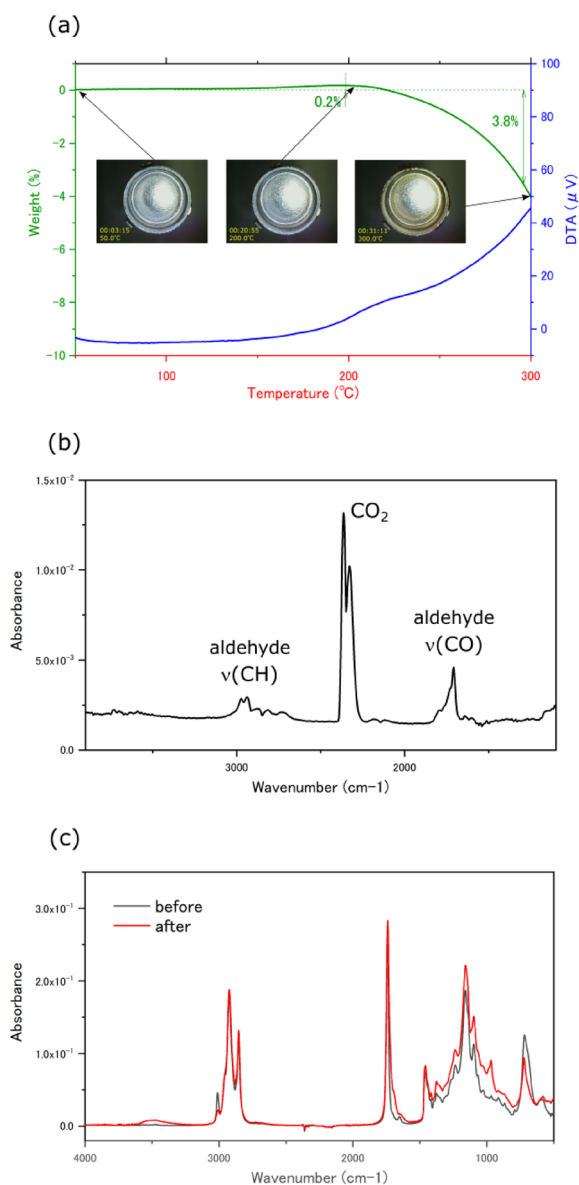


**Fig. 7.** (a) Sample observation TG-DTA of linseed oil, (b) IR spectrum of the evolved gases at 230°C, (c) IR spectra of linseed oil before and after TG-DTA measurement with ATR method.

nutritional value, the generation of a heated oil odor, and transformation into highly viscous, colored oils. Various methods, such as the peroxide value (PV)

method, are employed to analyze edible oils post-thermal oxidation<sup>(14)</sup>. However, few examples of real-time analysis of the thermal oxidation process exist<sup>(15)</sup>. Sample observation TG-FTIR is suitable for investigating thermal behaviors such as mass change, exo/endergonic reaction, color change, and reaction products.

Figure 7(a) presents the results of heating linseed oil to 300°C in a dry air atmosphere. The DTA curve shifted in the exothermic direction above 150°C, and the TG curve showed a slight mass gain at 150°C before a mass loss. The optical observation of the sample indicated a gradual yellowing. The IR spectrum of the gas evolved during mass loss at 230°C (Fig. 7(b)) exhibits bands assigned to CO<sub>2</sub> and aldehydes. It is hypothesized that the carbon chains of the unsaturated fatty acids in the linseed oil were oxidized to aldehydes, followed by cleavage of the chains and release as gas components.

FTIR can be applied not only in combination with TG but also with other attachments. Therefore, we used the attenuated total reflection (ATR) method to confirm the IR spectrum of linseed oil before and after heating, as shown in Fig. 7(c). After heating, an OH band of carboxylic acid appears at around 3500 cm<sup>-1</sup>, and the width of the low wavenumber side of the CO stretching vibration at around 1700 cm<sup>-1</sup> increases, indicating an increase in aldehydes and carboxylic acids. These behaviors suggest the progress of oxidation. Additionally, the change near 1000 cm<sup>-1</sup> indicates that unsaturated fatty acids transform from cis to trans due to heating, leading to an increase in harmful trans fatty acids<sup>(16)</sup>.

## 4. Inorganic Materials

### 4.1. Thermal Decomposition of Gypsum

Gypsum, a mineral primarily composed of calcium sulfate, offers numerous benefits and applications that can enhance various projects and industries. In the construction industry, it is utilized as gypsum board, an interior material for walls and ceilings in residential and commercial buildings, offering advantages such as fire resistance, fire prevention, and cost-effectiveness. Additionally, gypsum finds applications in artistic modeling, ceramic molding, metal and glass casting, civil engineering, and various products including medical casts, blackboard chalk, and food additives. In this study, gypsum dihydrate was heated to 1400°C in N<sub>2</sub> atmosphere and analyzed by TG-FTIR.

Figure 8(a) shows the TG-DTA and GS curves, and the IR spectra within the temperature range where these changes occur are shown in Fig. 8(b). In the temperature range from 100°C to 200°C, a 20% mass loss accompanied by an endothermic peak and a GS peak were observed. The IR spectrum detected H<sub>2</sub>O, indicating the dehydration of gypsum dihydrate. At 360°C, an exothermic peak was observed, indicating the crystal transformation from anhydrite III to anhydrite II. An endothermic peak at 1220°C indicates the crystal transformation from anhydrite II to anhydrite I. In

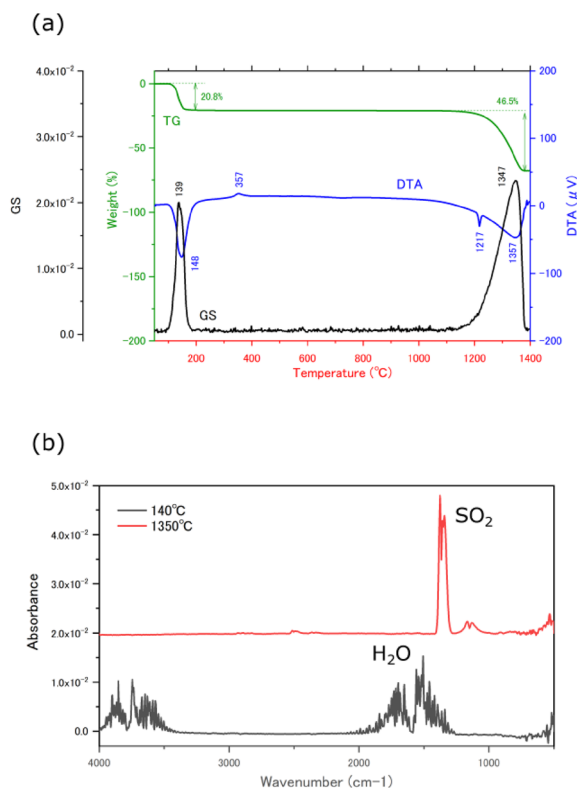


**Fig. 8.** TG-FTIR measurement of gypsum dihydrate. (a) TG-DTA and GS curves, (b) IR spectra at 140 and 1350°C.

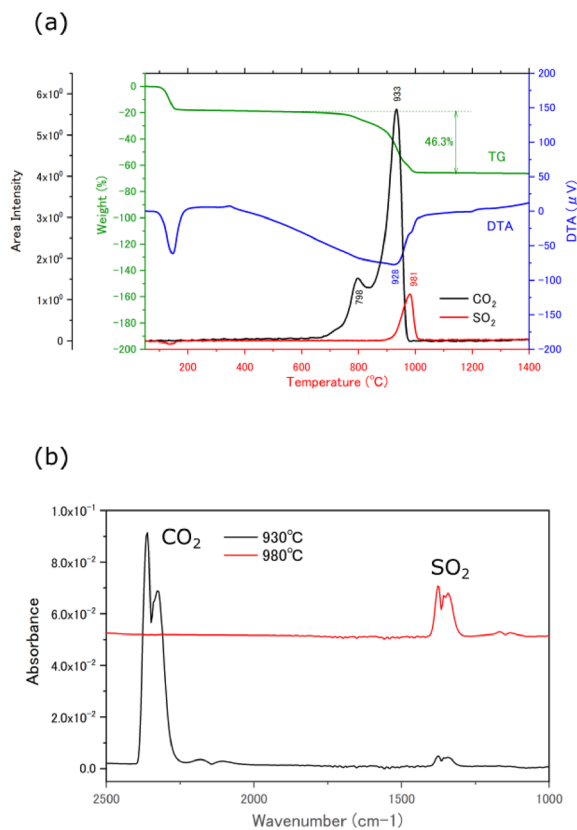


**Fig. 9.** TG-FTIR measurement of gypsum mixed with carbon powder. (a) TG-DTA and GS curves, (b) IR spectra at 930 and 980°C.

the temperature range from 1100 to 1400°C, a 47% mass loss, an endothermic peak, and a GS peak were observed. The IR spectrum revealed the evolution of SO<sub>2</sub>, indicating the thermal decomposition of anhydrite.

Carbon powder was mixed with gypsum dihydrate, and the mixture was heated under N<sub>2</sub> atmosphere. This method is applied in recycling waste gypsum boards, which involve converting it into calcium sulfide as an additive for lubricants and paints<sup>(17)–(19)</sup>. The results of TG-FTIR are shown in Fig. 9. Significant changes were observed in the temperature range from 700 to 1000°C, exhibiting a mass loss and an endothermic peak. The IR spectrum at this stage indicated the evolution of CO<sub>2</sub> at 930°C and SO<sub>2</sub> at 980°C (Fig. 9(b)). The area intensity of the absorption bands of these gases was extracted and overlaid on the TG-DTA curve (Fig. 9(a)), revealing the evolution of CO<sub>2</sub> followed by SO<sub>2</sub>. As shown in Equation (1), calcium sulfate reacts with carbon powder to produce calcium sulfide and CO<sub>2</sub>. Subsequently, calcium sulfide and calcium sulfate react to form calcium oxide and SO<sub>2</sub>, as shown in Equation (2).



## 5. Summary

TG-FTIR is effective for identifying reaction products in TG-DTA measurements. This paper has shown several applications of polymers, pharmaceuticals, foods, and inorganic materials. Numerous additional applications will be investigated soon.

## Acknowledgment

We are deeply grateful to Mitsuo Hattori of Thermo Fisher Scientific Co., Ltd. for his insightful advice on FTIR measurements and analysis throughout this study.

## References

- (1) S. Materazzi: *Appl. Spectrosc. Rev.*, **32** (1997), 385–404.
- (2) T. Arai: *Rigaku Journal*, **34** (2018), No. 2, 30–34.
- (3) Y. Nakanishi, M. Kimoto, and T. Awaji: *J. Soc. Mater. Sci. Jpn.*, **45** (1996), 1125–1130.
- (4) Y. M. Yun, M. W. Seo, G. H. Koo, H. W. Ra, S. J. Yoon, Y. K. Kim, J. G. Lee, and J. H. Kim: *Fuel*, **137** (2014), 321–327.
- (5) Y. Qiao, O. Das, S.-N. Zhao, T.-S. Sun, Q. Xu, and L. Jiang: *Polymers*, **12** (2020), 2739.
- (6) Y. Kobayashi: *J. Jpn. Soc. Precision Engineering*, **56** (1990), 634–638.
- (7) Y. Nakanishi, M. Kimoto, and T. Awaji: *J. Soc. Mater. Sci. Jpn.*, **45** (1996), 1125–1130.
- (8) K. Yoshitake and K. Tazumi: *Mater. Cycle. Waste Manag. Res.*, **34** (2023), 107–115.
- (9) L. C. K. Liao, T. C. K. Yang, and D. S. Viswanath: *Polym. Eng. Sci.*, **36** (1996), 2589–2600.
- (10) M. Minami, J. Tatami, M. Iijima, T. Takahashi, and T. Ohji: *Ceram. Int.*, **49** (2023), 15387–15394.
- (11) M. Beneš V. Plaček, G. Matuschek, A. Kettrup, K. Györyová, and V. Balek: *J. Appl. Polym. Sci.*, **99** (2006), 788–795.
- (12) L. Liu, D. Gong, L. Bratasz, Z. Zhu, and C. Wang: *Polym. Degrad. Stab.*, **168** (2019), 108952.
- (13) M. A. L. Pinto, B. Ambrozini, A. P. G. Ferreira, and É. T. G. Cavalheiro: *Braz. J. Pharm. Sci.*, **50** (2014), 877–884.
- (14) K. Ichikawa: *J. Nagoya Bunri Univ.*, **12** (2012), 121–130.

- (15) G. C. de Carvalho, M. de F. V. de Moura, H. G. C. de Castro, J. H. da Silva Júnior, H. E. B. da Silva, K. M. dos Santos, and Z. M. S. Rocha: *J. Therm. Anal. Calorim.*, **140** (2020), 2247–2258.
- (16) K. Fukuzumi: *J. Jpn. Oil Chem. Soc.*, **10** (1961), 143–146.
- (17) R. Naito, K. Fujimori, and M. Sugai: *J. Ceram. Assoc. Jpn.*, **77** (1969), 399–405.
- (18) N. Mihara, D. Kuchar, H. Matsuda, T. Iwashita, and K. Kyaw: *J. Soc. Inorg. Mater. Jpn.*, **14** (2007), 214–220.
- (19) M. Hashimura, Y. Toda, and Y. Yamamoto: *Proceedings of the Annual Conference of The Japan Society of Waste Management Experts*, **17** (2006), 177–177.